PHYSICAL REVIEW A **71**, 041802(R) (2005)

Demonstration of the spatial separation of the entangled quantum sidebands of an optical field

E. H. Huntington, G. N. Milford, and C. Robilliard
Centre for Quantum Computer Technology, School of Information Technology and Electrical Engineering, University College, The University of New South Wales, Canberra, Australian Capital Territory 2600, Australia

T. C. Ralph
Centre for Quantum Computer Technology, Department of Physics, The University of Queensland, St Lucia, Queensland 4072, Australia

O. Glöckl, U. L. Andersen, S. Lorenz, and G. Leuchs
Max-Planck-Forschungsgruppe, Institut für Optik, Information und Photonik, Universität Erlangen-Nürnberg, Günther-Scharowsky-Strasse, 1/Bau 24, 91058 Erlangen, Germany

(Received 14 April 2004; published 13 April 2005)

Quantum optics experiments on "bright" beams are based on the spectral analysis of field fluctuations and typically probe correlations between radio-frequency sideband modes. However, the extra degree of freedom represented by this dual-mode picture is generally ignored. We demonstrate the experimental operation of a device which can be used to separate the quantum sidebands of an optical field. We use this device to explicitly demonstrate the quantum entanglement between the sidebands of a squeezed beam.

DOI: 10.1103/PhysRevA.71.041802 PACS number(s): 42.50.Lc, 03.67.Mn

Early on in the discussion of squeezed light it was realized that a single-mode description is often not adequate. The spectral structure of squeezed light with its frequency sidebands is essential when analyzing specific Fourier components of the field fluctuations [1–4]. From a theoretical point of view it became clear that the two sidebands of a squeezed beam carry quantum correlated noise [1,3,5]. Later it was realized that squeezing across two distinct spatial modes led to entanglement and tests of the Einstein-Podolsky-Rosen (EPR) gedanken experiment using such two-mode squeezed light were proposed [6,7] and demonstrated [8–10]. Since then EPR entanglement has been recognized as a basic resource of continuous-variable quantum-information protocols [11]. Two-mode squeezing involves pairwise correlations between the four frequency sideband modes of the two beams. Recently it has been suggested that the spectral sideband correlations of single-mode squeezed light can be transferred to entanglement between two spatial modes [12,13]. The entanglement thus produced would be of a quite different character from that produced by two-mode squeezing as it would involve a pairwise correlation between only a single sideband on each of the beams.

In this Rapid Communication we demonstrate experimentally the production of this type of entangled light by separating the quantum sidebands of a single spatial mode into two separate spatial beams. We first demonstrate the basic effect using continuous-wave coherent states (experiment type *A*) and then demonstrate entanglement production from pulsed squeezed light (experiment type *B*). As well as the fundamental interest of demonstrating this paradigm of quantum optics explicitly, the techniques described here represent an additional tool in the analysis and manipulation of quantum optical fields [14,15] and produce entanglement useful for quantum-information applications. Note that the ability to detect a single sideband may also open further possibilities for astronomy [16].

Figure 1 illustrates our experimental setup. This figure also shows sketches of input and output frequency spectra indicating the desired operation of the system. The system is essentially a Mach-Zehnder interferometer whereby the path length for one of the interferometer arms is much greater than for the other, thus introducing a time delay between the two arms of τ. Previously such unbalanced Mach-Zehnder interferometers (UMZIs) have been used in quantum-optics experiments to filter spurious longitudinal lasing modes [17] and measure the phase quadrature of bright pulsed beams [18,19]. Here we pick the path-length difference such that the quantum sidebands at a particular radio frequency are decomposed into separate spatial beams.

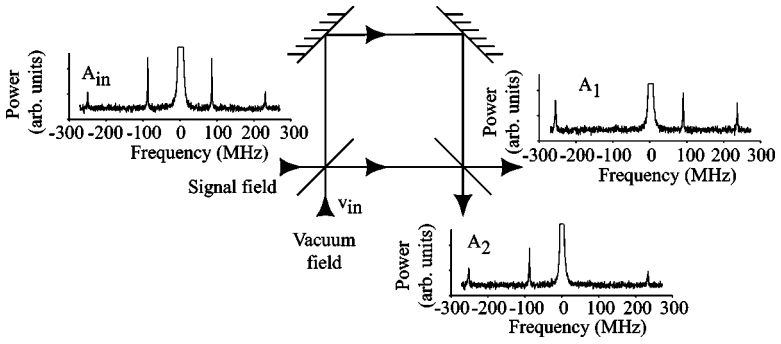

FIG. 1. A schematic diagram of the system along with spectra illustrating successful operation at the classical level. All the spectral measurements were made with a scanning confocal Fabry-Pérot cavity [21] with a free spectral range of 500 MHz and a linewidth of approximately 2 MHz. The truncated carrier is shown at zero frequency, the phase-modulation sidebands are at ± 90.5 MHz and residual mode-mismatch peaks (with less than 1% power) are at ± 250 MHz.

All of the beam splitters in the UMZI are assumed 50% transmitting. In the Heisenberg picture, time-varying fields are written in the rotating frame as $\hat{A}(t)=\overline{A}+\delta\hat{A}(t)$ and $\hat{A}(t)^\dagger=\overline{A^\star}+\delta\hat{A}(t)^\dagger$ where the steady-state coherent amplitude of the field is given by $\overline{A}$ and the time-varying component of the field is given by the operator $\delta\hat{A}(t)$. In Fourier-transform space, we may define operators for the quadrature amplitude and phase fluctuations of a field as $\delta X^+(\omega)=\delta A(\omega)+\delta A(-\omega)^\dagger$ and $\delta X^-(\omega)=i[\delta A(\omega)-\delta A(-\omega)^\dagger]$, respectively. The absence of carets indicates the Fourier transform. Additionally we have made use of the relation that $\delta\hat{A}(t)\rightarrow\delta A(\omega)\Rightarrow\delta\hat{A}(t)^\dagger\rightarrow\delta A(-\omega)^\dagger$ to find the relevant creation operators in the frequency domain [19]. The spectral variances $V^\pm$ of all fields are found from $\langle|\delta X^\pm(\omega)|^2\rangle$.

The annihilation operators for the UMZI inputs (outputs) at a Fourier frequency ω relative to the carrier are denoted $\delta A_{\rm in}(\omega)$ and $\delta v_{\rm in}(\omega)$ [$\delta A_1(\omega)$ and $\delta A_2(\omega)$] (see Fig. 1). The outputs of the UMZI are given in terms of the inputs as

$$\delta A_{1,\phi}(\omega)=\frac{1}{2}[\delta A_{\rm in}(\omega)(1-e^{i\phi}e^{i\omega\tau})+i\delta v_{\rm in}(\omega)(e^{i\phi}e^{i\omega\tau}+1)], \tag{1}$$

$$\delta A_{2,\phi}(\omega)=\frac{1}{2}[i\delta A_{\rm in}(\omega)(e^{i\phi}e^{i\omega\tau}+1)+\delta v_{\rm in}(\omega)(e^{i\phi}e^{i\omega\tau}-1)], \tag{2}$$

where $\phi=2m\pi+\omega_0\tau=\omega_0\tau$ is the phase shift acquired by a field at the carrier frequency ω_0. Let us focus on the specific frequency Ω such that $\Omega\tau=\pi/2$. Choosing $\phi=+\pi/2$, the outputs of the UMZI are

$$\delta A_{1,+\pi/2}(\Omega)=\delta A_{\rm in}(\Omega),\quad \delta A_{1,+\pi/2}(-\Omega)=i\delta v_{\rm in}(-\Omega),$$

$$\delta A_{2,+\pi/2}(\Omega)=-\delta v_{\rm in}(\Omega),\quad \delta A_{2,+\pi/2}(-\Omega)=i\delta A_{\rm in}(-\Omega).$$

For $\phi=-\pi/2$ the $\pm\Omega$ terms are interchanged.

Hence we find that the positive and negative frequency components of the input field can be separated into spatially distinct beams. If the UMZI is locked to $-\pi/2$ the upper and lower sidebands will exit from the opposite ports. This behavior has been confirmed experimentally and is indicated in Fig. 1. The spectra illustrating successful operation at the classical level are the results of measurements of a continuous-wave neodymium-doped yttrium aluminum garnet (Nd:YAG) laser (Innolight Mephisto 500) with 90.5 MHz phase modulation sidebands sent as an input to the UMZI (experiment type *A*). The UMZI had a path-length difference of 0.83 m and fringe visibility of 98%. The dc power at output A_1 was used to lock the interferometer. Spectral measurements of the field A_2 were made for $\phi=+\pi/2$ and $-\pi/2$. The second of these is shown on the A_1 output to illustrate schematically the desired operation of the device. The spatial separation of the upper and lower sidebands is clearly visible.

We now turn to nonclassical effects. The power spectrum

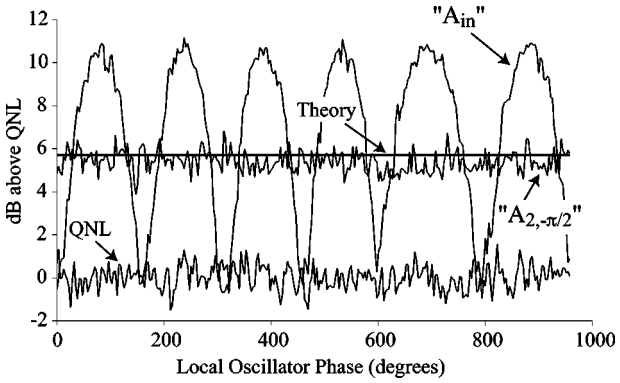

FIG. 2. Homodyne measurements of the quantum noise limit (QNL) for the local oscillator power; the input to the UMZI ("$A_{\rm in}$"), one output of the UMZI when locked to $\phi=-\pi/2$ ("$A_{2,-\pi/2}$"); and the predicted output of the UMZI based on the measured input amplitude and quadrature phase variances, as well as the measured homodyne detection fringe visibilities (0.89% and 0.92% for input and output, respectively [20]) and UMZI fringe visibility ("Theory").

of the input fluctuations is given by

$$V_{\rm in}^\pm=\langle\delta A_{\rm in}(\Omega)^\dagger\delta A_{\rm in}(\Omega)+\delta A_{\rm in}(-\Omega)^\dagger\delta A_{\rm in}(-\Omega)\pm\delta A_{\rm in}(-\Omega)\delta A_{\rm in}(\Omega)\pm\delta A_{\rm in}(-\Omega)^\dagger\delta A_{\rm in}(\Omega)^\dagger\rangle+1. \tag{3}$$

The final unit component in the sum is the vacuum noise. Using the transfer relations for the UMZI ($\phi=+\pi/2$) we find for the output fluctuations of the first beam

$$V_{\rm out1}^\pm=\langle\delta A_{\rm in}(\Omega)^\dagger\delta A_{\rm in}(\Omega)\rangle+1, \tag{4}$$

where expectation values such as $\langle\delta v_{\rm in}^\dagger\delta v_{\rm in}\rangle$, $\langle\delta A_{\rm in}^\dagger\delta v_{\rm in}^\dagger\rangle$, and $\langle\delta A_{\rm in}\delta v_{\rm in}\rangle$ are all zero. $V_{\rm out2}^\pm$ is similar to Eq. (4) with Ω replaced by $-\Omega$. Thus we expect only the power of the upper sideband to appear at the first output and only that of the lower sideband to appear at the second. Also we expect the spectra to be independent of the local oscillator phase when probing the sidebands with a homodyne detector. If the input state is symmetric (same power in the upper and lower sidebands) then the variances of the amplitude and phase quadratures of both outputs of the UMZI when locked to either $\pm\pi/2$ would be [normalized to the quantum noise limit (QNL) of one output]

$$V_{\rm out}=(V_{\rm in}^+ + V_{\rm in}^- + 2)/4. \tag{5}$$

Figure 2 shows the results of homodyne measurements of the input and output of the UMZI for experiment type *A* at 90.5 MHz. Reference [14] outlines the approach taken to model mode mismatch. To take an example, the intensity noise of either of the output fields is $V_{\rm out,MM}^+=(V_{\rm in}^+ + \eta_{\rm MM}V_{\rm in}^- + 3-\eta_{\rm MM})/4$ where $\eta_{\rm MM}$ is the mode-matching efficiency of the UMZI given by the square of the fringe visibility. There is good agreement between the measured and predicted behavior of the UMZI.

Of more interest is what happens if the input beam is squeezed. From Eq. (5) we see that the noise of the output

beam must be greater than the QNL for all quadratures (as $V+1/V$ is always greater than 2 for $V\neq 1$). Indeed, from Eq. (4), this shows that squeezed beams have sideband photons. So the output beams show excess noise. Now consider the correlations between the output beams. If amplitude quadrature measurements are simultaneously made on both beams then the sum and difference photocurrent variances (normalized to the QNLs of both output beams) are given by

$$V^{+}_{\mathrm{add}} = (V^{+}_{\mathrm{in}} + 1)/2, \quad V^{+}_{\mathrm{sub}} = (V^{-}_{\mathrm{in}} + 1)/2. \tag{6}$$

If the input beam is amplitude squeezed then Eq. (6) shows that amplitude measurements of the two beams are anticorrelated to below the QNL. On the other hand if phase quadrature measurements are simultaneously made on both beams then the normalized sum and difference photocurrent variances are given by

$$V^{-}_{\mathrm{add}} = (V^{-}_{\mathrm{in}} + 1)/2, \quad V^{-}_{\mathrm{sub}} = (V^{+}_{\mathrm{in}} + 1)/2. \tag{7}$$

Thus phase quadrature measurements are correlated to below the QNL. Sub-QNL correlations on both quadratures are the signature of entanglement [22], showing that the sideband entanglement has been transferred to entanglement between spatially separated beams [12].

To demonstrate these quantum effects, we use an UMZI to separate the sidebands of an amplitude-squeezed input field. In this experiment (type *B*), we use a commercially available pulsed optical parametric oscillator pumped by a mode-locked Ti:sapphire laser (both Spectra Physics). The optical parametric oscillator produces pulses of 130 fs at a center wavelength of 1530 nm and a repetition rate of 82 MHz. The nonlinear Kerr effect experienced by intense pulses in optical fibers (see, e.g., Ref. [23]) is used to generate nonclassical states of light. During propagation of such pulses through a fiber, a high degree of excess phase noise is introduced mainly due to some classical noise effects. Employing an asymmetric fiber Sagnac interferometer [24], amplitude squeezing can be produced, the amplitude not being affected by excess noise.

For a pulsed laser beam the separation of sidebands can be performed only at certain frequencies, as two conditions have to be satisfied simultaneously: (1) Two pulses have to overlap temporally giving a boundary condition for the path-length difference $\Delta L = cnT_{\mathrm{rep}}$ (n is an integer number and T_{rep} is the time between two pulses) and (2) a $\pi/2$ phase shift at the measurement frequency f_m must be introduced, so that $\Delta L = c/(4f_m)$. Possible measurement frequencies are therefore $f_m = 1/(4nT_{\mathrm{rep}})$. At our repetition rate the arm-length difference must be a multiple of 3.66 m, corresponding to the distance between two successive pulses. The arm-length difference is set to be 7.32 m for measurements at 10.25 MHz.

We launched about 4 dB of amplitude-squeezed light into the UMZI. A visibility of 95% was observed at the output to generate entanglement. On each of the two output beams we performed an amplitude noise measurement (see the upper two graphs in Fig. 3). The amplitude noise of the output beams (gray traces) is almost 20 dB above the quantum noise limit (black traces). This high noise level is an indication that strong correlations between pairs of sidebands might be present. Note also that the squeezing is lost as a result of the separation of sidebands. The high noise level is not only due to antisqueezing, but also due to the high classical thermal phase noise of our squeezed states.

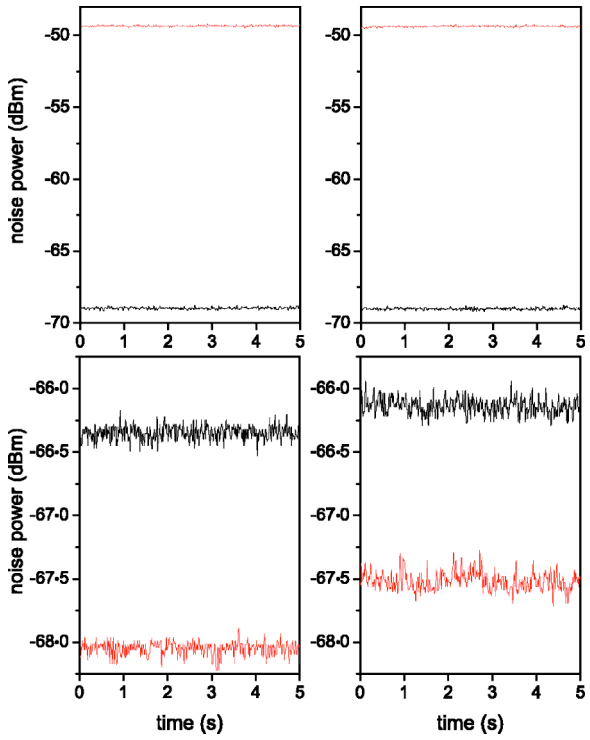

FIG. 3. Characterization of the output beams of the UMZI when using squeezed light. The upper two graphs show the amplitude noise level of the individual beams (gray lines) compared to the respective quantum noise limit (black lines). The lower left graph shows the correlations in the amplitude quadrature (gray line) compared to the quantum noise limit (black line). The lower right graph shows the correlations in the phase quadrature (gray line) compared to the quantum noise limit (black line). All noise levels have been detected using a pair of spectrum analyzers (HP 8590) at a measurement frequency of 10.25 MHz, a resolution bandwidth of 300 kHz, and a video bandwidth of 30 Hz. All traces have been corrected for the electronic noise level, which was at about −77.9 dB m.

To demonstrate that this beam pair is indeed entangled, correlations below the quantum noise limit between the two beams in the amplitude as well as in the phase quadrature must be observed. While amplitude correlations are verified rather easily in direct detection of the two output modes and subsequent correlation of the photocurrents, phase measurements are more involved. Having intense pulsed light trains, neither homodyne detection (which might saturate our detectors due to the high intensities involved) nor phase-shifting cavities (with high requirements on resonance conditions) could be easily employed. We therefore used an interferometric scheme where two entangled beams interfere at yet another 50-50 beam splitter. Their relative phase is such that the output beams (denoted *a* and *b*) of this interference have equal intensity [10]. Both output beams are then detected directly. The spectral component at frequency ω of the sum and the difference of the photocurrents from the two detectors yields signals that are proportional to the sum of the

amplitude and the difference of the phase quadratures of the two entangled beams, respectively,

$$V[\delta n_a(\omega) + \delta n_b(\omega)] = V[\delta X_1^+(\omega) + \delta X_2^+(\omega)] = V_{\text{add}}^+,$$

$$V[\delta n_a(\omega) - \delta n_b(\omega)] = V[\delta X_1^-(\omega) - \delta X_2^-(\omega)] = V_{\text{sub}}^-.$$

The measurement scheme is equivalent to a Bell-state measurement on intense light beams [25]. It turned out that this type of measurement can also be applied to the entangled beam pair generated by separating the sidebands to check for the correlations in the amplitude and the phase quadrature. In the verification experiment, we achieved a visibility of more than 90%. We observed about 1.6 dB of correlations below the quantum noise limit in the amplitude quadrature (lower left traces in Fig. 3) and about 1.4 dB of correlations in the phase quadrature (lower right traces in Fig. 3). This experiment shows that the quantum correlations between the sidebands of the squeezed input beam have been successfully transferred to quantum correlations between two spatially distinct outputs. The result clearly shows the entanglement between the outputs, as nonclassical correlations in both the amplitude as well as the phase quadrature of the beam pair were detected. Note that the degree of observed correlations of 1.6 dB for the amplitude quadrature (1.4 dB for the phase quadrature) agrees with the prediction from theory. About 1.6 dB of correlations are expected when 4 dB of input squeezing are used, as the correlations are degraded by the contribution of the uncorrelated vacuum sidebands [see Eqs. (6) and (7)]. To extract the full correlations of 4 dB a pair of frequency-shifted local oscillators would have to be applied as proposed by Zhang [13].

In summary, we have demonstrated the production of a different type of entangled light via a device that can be used to separate the quantum sidebands of an optical field. This device is in essence an unbalanced Mach-Zehnder interferometer where the path-length difference is determined by the frequency at which sideband separation is required. We have shown that the UMZI may be used to spatially separate the positive and negative sidebands of a phase-modulated optical field. Applying this to single-mode squeezed light produces spatially separated entangled beams. Many landmark experiments have investigated quantum properties with homodyne detection, for example, [26,27]. The techniques described here and in Ref. [14] open another window on these and other quantum-optics experiments.

This work was supported by the Australian Research Council and by the Schwerpunktprogramm 1078 of the Deutsche Forschungsgemeinschaft and the network of competence QIP of the State of Bavaria (A8). U.A. gratefully acknowledges financial support of the Alexander von Humboldt foundation.

[1] C. M. Caves, Phys. Rev. D **26**, 1817 (1982).
[2] W. G. Unruh, in *Quantum Optics, Experimental Gravitation, and Measurement Theory*, edited by P. Meystre and M. O. Scully (Plenum, New York, 1983), p. 647.
[3] C. M. Caves and B. L. Schumaker, Phys. Rev. A **31**, 3068 (1985).
[4] B. Yurke, Phys. Rev. A **32**, 300 (1985).
[5] J. Gea-Banacloche and G. Leuchs, J. Mod. Opt. **34**, 793 (1987).
[6] R. Graham, Phys. Rev. Lett. **52**, 117 (1984).
[7] M. D. Reid and P. D. Drummond, Phys. Rev. Lett. **60**, 2731 (1989); M. D. Reid, Phys. Rev. A **40**, 913 (1989).
[8] Z. Y. Ou *et al.*, Phys. Rev. Lett. **68**, 3663 (1992); S. F. Pereira *et al.*, Phys. Rev. A **62**, 042311 (2000).
[9] Y. Zhang *et al.*, Phys. Rev. A **62**, 023813 (2000).
[10] Ch. Silberhorn *et al.*, Phys. Rev. Lett. **86**, 4267 (2001).
[11] *Continuous Variable Quantum Information*, edited by S. Braunstein and A. Pati (Kluwer Academic Publishers, Dordrecht, 2003).
[12] E. H. Huntington and T. C. Ralph, J. Opt. B: Quantum Semiclassical Opt. **4**, 123 (2002).
[13] J. Zhang, Phys. Rev. A **67**, 054302 (2003).
[14] E. H. Huntington and T. C. Ralph, Phys. Rev. A **69**, 042318 (2004).
[15] J. M. Merolla *et al.*, Phys. Rev. Lett. **82**, 1656 (1999).
[16] M. A. Johnson and C. H. Townes, Opt. Commun. **179**, 183 (2000).
[17] S. Inoue *et al.*, J. Opt. Soc. Am. B **14**, 2761 (1997).
[18] O. Glöckl *et al.*, Opt. Lett. **29**, 1936 (2004).
[19] R. J. Glauber, Phys. Rev. **130**, 2529 (1963).
[20] H. A. Bachor and T. C. Ralph, *A Guide to Experiments in Quantum Optics*, 2nd ed. (Wiley-VCH, Wenheim, 2003).
[21] H. Kogelnik and T. Li, Appl. Opt. **5**, 1550 (1966).
[22] L.-M. Duan *et al.*, Phys. Rev. Lett. **84**, 2722 (2000); R. Simon, *ibid.* **84**, 2726 (2000).
[23] A. Sizmann and G. Leuchs, Prog. Opt. **39**, 373 (1999).
[24] S. Schmitt *et al.*, Phys. Rev. Lett. **81**, 2446 (1998); D. Krylov and K. Bergman, Opt. Lett. **23**, 1390 (1998).
[25] G. Leuchs *et al.*, J. Mod. Opt. **46**, 1927 (1999); J. Zhang and K. Peng, Phys. Rev. A **62**, 064302 (2000).
[26] G. Breitenbach and S. Schiller, Nature (London) **387**, 471 (1997).
[27] A. Furusawa *et al.*, Science **282**, 706 (1998).